agronomy

MDPI

Article

Insights into the Photosynthetic Efficiency and Chloroplast Ultrastructure of Heat-Stressed Edamame Cultivars During the Reproductive Stages

Makoena Joyce Moloi [1], Csilla Tóth [2], Arslan Hafeez [3] and Brigitta Tóth [4,*]

[1] Department of Plant Sciences-Botany Division, Faculty of Natural and Agricultural Sciences, University of the Free State, 205 Nelson Mandela Drive, Park West, Bloemfontein 9301, South Africa; moloimj@ufs.ac.za
[2] Department of Agricultural Sciences and Environmental Management, Institute of Engineering and Agricultural Sciences, University of Nyíregyháza, Sóstói Str. 31/b, H-4400 Nyíregyháza, Hungary; toth.csilla@nye.hu
[3] Department of Botany, Government College University, Faisalabad 38000, Pakistan; arslanhafeezuaf@gmail.com
[4] Institute of Food Science, Faculty of Agricultural and Food Sciences and Environmental Management, University of Debrecen, Böszörményi Str. 138, H-4032 Debrecen, Hungary
* Correspondence: btoth@agr.unideb.hu

Abstract: High temperatures have adverse impacts on the photosynthetic efficiency and yield of many crop plants. This study investigated how high temperatures affect the photosynthetic efficiency parameters and chloroplast ultrastructure of three edamame cultivars (AGS354, UVE17, and UVE14) at the reproductive stages (flowering and pod-filling). Heat stress (HS) treatments were performed under controlled conditions in climate chambers set at 25/18 °C (control), 30/23 °C (HS-I), and 35/28 °C (HS-II). The AGS354 cultivar exhibited the greatest susceptibility under HS-II treatment, characterised by a reduction in the photochemical reactions, decreased chlorophyll-a (chl-a) and carotenoid accumulation, the highest increase in the starch grain traits, and reduced plastoglobule and grana area traits. In UVE 14 and UVE17, the HS-II treatment enhanced chl-a and chl-b accumulation. Elevated carotenoid levels in UVE14 and UVE17 likely protected chlorophyll from degradation and mitigated photooxidative damage. The HS-II treatment also enhanced the grana traits, supporting improved light-harvesting capacity during heat stress in UVE14 and 17. However, heat stress disrupted the photochemical reactions (quantum efficiency of photosystem II, performance index absorbance, and performance index), indicating that elevated carotenoids alone do not exhibit complete tolerance to heat stress. Since plastoglobules play an essential in carotenoid biosynthesis, increased or stabilised plastoglobule traits in UVE14 and UVE17 under HS-II treatment strongly indicate improved heat stress tolerance. Overall, UVE14 and UVE17 emerged as the most heat-tolerant cultivars, with AGS354 being the most susceptible. These findings provide valuable insights into heat stress adaptation mechanisms and suggest the UVE14 and UVE17 cultivars as potential candidates for breeding heat-tolerant edamame cultivars.

Keywords: chlorophyll; chloroplast ultrastructure; heat stress; photosynthesis; vegetable-type soybeans

Academic Editor: Guanfu Fu

Received: 29 November 2024
Revised: 22 January 2025
Accepted: 23 January 2025
Published: 25 January 2025

Citation: Moloi, M.J.; Tóth, C.; Hafeez, A.; Tóth, B. Insights into the Photosynthetic Efficiency and Chloroplast Ultrastructure of Heat-Stressed Edamame Cultivars During the Reproductive Stages. *Agronomy* **2025**, *15*, 301. https://doi.org/10.3390/agronomy15020301

1. Introduction

Vegetable-type soybean, also known as edamame, *Glycine max* (L.) Merr. is a well-known legume crop in Asia and America, but in Africa, it is considered relatively new and

underutilised [1,2]. In South Africa, edamame was introduced in 2009 by the Edamame Development Program; however, its cultivation area is still small. Edamame is a good source of complete protein as it contains all eight essential amino acids. In addition to protein, it is rich in various vitamins, minerals, isoflavones, fibre, magnesium, and folate. The literature also suggests that edamame may offer health benefits [3]. Rising global temperatures, driven by increased greenhouse gas emissions, significantly threaten crop productivity [4,5]. It is projected that temperatures will increase by 1.4–3 °C (2050) and 2–3 °C (2100) [6]. Although a 1 °C temperature increase may seem minor, it can significantly reduce soybean yields by up to 17% [7].

High temperatures negatively impact physiological processes such as photosynthesis, particularly in C3 plants. One of the contributing factors is that Rubisco, which has a low affinity for carbon dioxide (CO_2) under high temperatures, activates photorespiration, an energy-wasteful process that affects plants and inhibits photosynthesis and plant growth [8]. In addition, high temperatures can dissociate the oxygen-evolving complex (OEC), reduce the supply of electrons to the light-dependent electron transport chain, inhibit the maximum quantum efficiency of the photosystem (PS) II reaction centre (Fv/Fm), reduce chlorophyll (chl)-a (chl-a) and chl-b, and reduce the chl-a/b ratio in plants [9]. Photosystem II (PSII) is the most heat-sensitive component of photosynthesis. It plays a critical role in the light-dependent reactions of photosynthesis, where it is responsible for splitting water molecules (photolysis) to release oxygen, protons, and electrons [10]. In grain-type soybeans, heat stress introduced at flowering reduced the leaf photosynthesis rate, stomatal conductance (SC), stomatal density, Fv/Fm, and photochemical quenching (PQ), increased non-photochemical quenching (NPQ), and damaged the chloroplasts, resulting in reduced seed yield and plant health [11,12].

Since photosynthesis occurs in the chloroplasts, maintaining the integrity of their ultrastructure is essential for regulating the light-dependent reactions, which in turn determine the photosynthetic performance of crops under various environmental conditions [11,13]. The suitable parameters for understanding the effects of heat stress on the ultrastructural changes of the chloroplast include the shape and the size of chloroplast, the number, area, and structure of grana, the number and size of starch grains, and the number and size of plastoglobules [11,13,14]. In grain-type soybeans, heat stress increased the size of the mesophyll chloroplast [15]. The changes at an ultrastructural level under heat stress are frequently driven by the excessive production of the reactive oxygen species (ROS) in the chloroplasts, which oxidise the lipids and proteins in the thylakoids [12]. Such oxidations compromise the integrity of the thylakoid membranes, inhibiting the photochemical processes [16,17]. The ROS could cause the plastoglobules to swell [18,19] or release lipids, leading to their shrinkage to protect the plants [20]. Zhang et al. [21] reported similar chloroplast swelling and plastoglobule changes in Arabidopsis under heat stress. Moreover, heat stress could cause chloroplast envelope damage, swelling of the thylakoids, less stacked thylakoids, obscure granum and stroma lamellae, and enlarged starch grains, reflecting poor photosynthetic status [15,17]. The inhibition of photosynthesis reduces the assimilation of the reducing sugars, leading to more starch storage and increased starch size [17]. In grain-type soybeans, heat stress reduced grana stacking [22], leading to reduced efficiency of light-dependent reactions. Herritt et al. [13] also showed that the chloroplast ultrastructural responses were influenced by the genotype and the duration of exposure to heat stress in grain soybeans. Djanaguiraman et al. [11] emphasised that a plant's developmental stage significantly affects its photosynthetic response.

Although edamame is consumed worldwide, there is still limited research on its responses to environmental stresses, particularly heat stress. Most studies are conducted on grain soybeans, and they focus on the photosynthetic responses under short-term

heat exposure at either vegetative or flowering stages. Expanding knowledge to examine the effects of heat stress on the photosynthetic responses across all reproductive stages, flowering and pod-filling, would significantly enhance our understanding, as the current literature lacks comprehensive records on this topic in edamame. Current research on edamame has primarily focused on drought stress or the combined effects of drought and heat stress [23,24], leaving a gap in understanding the specific impacts of heat stress alone on photosynthesis during both reproductive stages. Given the varying drought tolerances among edamame cultivars AGS354 (susceptible), UVE14 (tolerant), and UVE17 (susceptible) [25], it is crucial to assess their photosynthetic performance under high-temperature conditions. Similarly, under combined drought and heat stress, UVE14 had higher photosynthetic efficiency compared to UVE17 [24]. Considering the challenges associated with rising global temperatures, identifying heat-tolerant edamame cultivars is very important, which could enhance breeding programs focused on improving heat resilience. In addition, stable photosynthetic parameters under heat stress may serve as reliable criteria for selecting suitable heat-tolerant cultivars. Therefore, the goal of this study was to examine the effects of heat stress when applied at both reproductive stages (flowering and pod-filling) on the photosynthetic efficiency of three edamame cultivars (AGS354, UVE14, and UVE17) introduced in South Africa. These findings can inform targeted breeding to enhance edamame resilience in challenging climates, thus contributing to food security.

2. Materials and Methods

2.1. Plant Material, Experimental Setup, and Sampling

Three edamame cultivars (UVE17, AGS354, and UVE14 originating from the South African Edamame Development Program, KwaZulu-Natal) were germinated in seedling trays. Each tray contained 12 seeds per cultivar, with 1 seed planted per cell, using Hygromix seedling mix (Hygrotech, Pretoria, South Africa). The trays were kept in a greenhouse under controlled conditions, maintaining a daytime temperature of 25 °C and a nighttime temperature of 18 °C. Once the seedlings reached the unifoliate leaf stage, they were transplanted. Due to the lack of information on the responses of South African edamame cultivars to moderately elevated temperatures, cultivars were selected based on their drought tolerance. This selection allows for evaluating whether a drought-tolerant cultivar could potentially exhibit tolerance to both drought and heat stress, and whether a drought-susceptible cultivar might tolerate heat. AGS354 is high-yielding edamame that shows significant yield reduction under drought; UVE17 is also drought-susceptible and low-yielding, while UVE14 is drought-tolerant but low-yielding [25].

The seedlings (one seedling per pot) were planted in 9 L pots containing 10 kg dry red loamy sandy soil, which was irrigated to optimum water holding capacity as established by Moloi and van der Merwe [23]. Three growth chambers were set at different temperature treatments (control: 25/18 °C, heat stress (HS)-I: 30/23 °C, HS-II: 35/28 °CI) to assess the effects of heat stress on the photosynthetic efficiency of three edamame cultivars. Given the importance of the reproductive stages for crop yields, plants were exposed to these temperature treatments throughout the flowering (8 days) and pod-filling (8 days) stages. After each stage, plants were returned to the greenhouse at 25/18 °C. The pots were arranged using a completely randomised, split-plot design where the main plot was the three temperature treatments (control, HS-I, and HS-II) and the sub-plot was the cultivars (AGS354, UVE17, and UVE14). The design included three biological replications per cultivar and treatment, with four pots per plot. Since soybeans are known to tolerate temperatures up to 30 °C, the minimum temperature (night) was raised to induce heat

stress. The control treatment of 25/18 °C aligns with the optimal temperatures for soybean production in South Africa [26].

Sampling was conducted for each of the four pots within each replicate, targeting young, fully expanded trifoliate leaves eight days after exposure to each temperature treatment at the flowering and pod-filling stages. It was important to sample at these stages because although high-temperature stress can directly affect physiological processes and alter growth and development, the response depends on the sensitivity of the growth phase [27]. Leaf data sampling was conducted using both non-destructive and destructive methods. In the non-destructive approach, data were collected in vivo without removing the leaves, with data from each pot (trifoliate) within a replicate averaged to represent that replicate. For destructive measurements, the harvested trifoliate leaves from each pot within a replicate were combined and homogenised to represent a single replicate in the analysis. For chloroplast ultrastructure measurements, a method described by Spurr [28] was used to prepare the leaf samples for transmission electron microscopy (TEM). Leaf discs (0.5 cm diameter) were sampled from young, fully expanded leaves (same used for other photosynthetic parameters) at the pod-filling stage and immediately fixed in 0.1 M sodium phosphate buffer (pH 7.0) containing 3% (v/v) glutardialdehyde.

2.2. Non-Destructive Measurements

Sampling for the chlorophyll fluorescence parameters was performed at the flowering and pod-filling stages between 10:00 a.m. and noon, according to Hlahla et al. [24]. The Pocket photosynthetic efficiency analyser (PEA) instrument (Hansatech Instrument, King's Lynn, UK) was attached to leaf clips on the young, fully expanded trifoliate leaves following a 30 min dark adaptation. A saturating light (3000 µmol $m^{-2}s^{-1}$) was used to initiate the photochemical reactions. These measurements aimed to assess the impact of heat on several parameters, including the maximum quantum efficiency of photosystem II (Fv/Fm), the performance index (potential) for energy conservation from exciton to the reduction of intersystem electron acceptors (PIabs), and the performance index (potential) for energy conservation from exciton to the reduction of PSI end acceptors (PItot).

Stomatal conductance was measured using a leaf porometer, a device from Li-Cor (ADC Bioscientific Ltd., Hoddesdon, UK). This instrument quantifies the humidity gradient between the leaf chamber and its surroundings, thereby providing data for stomatal conductance (SC). The leaf porometer's sensor was placed on the underside of the leaf, where stomata are concentrated, for more accurate SC measurements. The measurements were taken between 10:00 a.m. and noon.

2.3. Destructive Measurements

2.3.1. Determination of the Photosynthetic Pigments and Total Soluble Sugar Contents

After sampling, the homogenised leaves from each pot (as described in Section 2.1) were crushed to a fine powder in liquid nitrogen and stored at −20 °C for quantification of the photosynthetic pigments (chl-a, chl-b, and carotenoids) and TSS. Pooling the leaves from each pot was necessary to ensure a representative sample of the plant material, as variability in photosynthetic pigment content and total soluble sugars (TSSs) can occur across individual plants within a pot. Homogenising and crushing the leaves minimised the sampling errors and ensured the consistency of the analysis. For measurement of the photosynthetic pigments, frozen leaf tissue (100 mg) was homogenised in 2 mL of 80% (v/v) ice-cold acetone (Sigma-Aldrich, Saint Louis, MO, USA) and centrifuged (5000× g for 5 min at 4 °C), and the resulting supernatant was used for the quantification of chl-a, chl-b, and carotenoids according to a method described by Pareek et al. [29].

Total soluble sugars (TSSs) were extracted and quantified following Irigoyen et al. [30]. Frozen leaf powder (0.1 g) was homogenised in 96% (*v*/*v*) ethanol, incubated at 80 °C for 10 min, and then centrifuged at 4000× *g* for 10 min at 4 °C. The supernatant (50 µL) was mixed with 1450 µL Anthrone reagent (1.5 mg/mL in 72% (*v*/*v*) sulfuric acid), vortexed, and incubated at 80 °C for 15 min. Absorbance was measured at 625 nm (Cary 100 Bio, Varian, Belrose, Australia), and the TSS concentration was calculated from a glucose standard.

2.3.2. Chloroplast Ultrastructure Assessments

After sampling (as described in Section 2.1), the leaves were further fixed overnight in 0.1 M sodium phosphate buffer (pH 7.0) containing 3% (*v*/*v*) glutardialdehyde at room temperature. Samples were subsequently post-fixed with 1% (*m*/*v*) osmium tetroxide in the same buffer for 2 h at room temperature and dehydrated in a graded acetone series before being embedded in Spurr epoxy resin. Ultrathin sections (100 nm thickness) were cut from the samples using a Leica ultramicrotome EM UC7 (Vienna, Austria). Sections were stained with uranyl acetate and lead citrate and then examined under a Philips CM100 TEM (FEI, Amsterdam, The Netherlands) at various magnifications (1450×, 13,500×, and 25,000×) to observe the mesophyll cells and chloroplasts. Sections/TEM samples were viewed using a Philips CM100 TEM at an acceleration voltage of 80 kV, and images were captured with a side-mounted Megaview III Camera (Soft Imaging System, Münster, Germany), using analySIS software (version 1).

The following micromorphometric parameters were examined: mesophyll cell size (µm^2), number of chloroplasts (No.) (each chloroplast in the mesophyll cell was counted and summed up), chloroplast length (µm), chloroplast width (µm), total chloroplast area (µm^2) (the area of every chloroplast was measured and totalled in each examined mesophyll cell), average chloroplast area (µm^2) (the total area of chloroplast was divided by the number of chloroplasts for each mesophyll cell), chloroplast cover index (%) (the chloroplast area was divided by the mesophyll cell area and multiplied by 100), total grana number per chloroplast (No.) (each granum was counted and totalled in the examined chloroplasts), total grana area (µm^2) (the area of all grana was measured and summed per chloroplast), average grana area (µm^2) (total grana area was divided by the number of grana in chloroplast), percent grana area (%) (the total grana area was divided by the chloroplast area and multiplied by 100), grana height (µm), number of grana lamellas (No.), grana lamella/lumen thickness (µm), total number of starch grains per chloroplast (No.) (the number of starch grains present in each chloroplast was counted), total starch grain area (µm^2) (the area of every starch grain was measured and totalled in every examined chloroplast), average starch grain area (µm^2) (the total area of starch grains was divided by the number of starch grains for each chloroplast), percent starch grain area (%) (the total starch grain area was divided by the chloroplast area and multiplied by 100), starch grain length (µm), starch grain width (µm), total number of plastoglobules per chloroplast (No.) (the number of plastoglobules present in each chloroplast was counted), total plastoglobule area (µm^2)) (the area of every plastoglobule was measured and totalled in every examined chloroplast), average plastoglobule area (µm^2) (the total area of plastoglobules was divided by the number of plastoglobules for each chloroplast), percent plastoglobule area (%) (the plastoglobule area was divided by the chloroplast area and multiplied by 100), plastoglobule height (µm), plastoglobule width (µm). A VSI RZ302 measuring program was used to measure the above micromorphometric parameters. The examined micromorphometric parameters were measured and digitally archived at 6000× (for complete mesophyll cell), 8000× and 11,500× (for complete chloroplast), and 66,000× (for grana) magnifications. For data reliability, ten chloroplasts were examined per cultivar and treatment, and the averages of the resulting traits were recorded.

2.4. Statistical Analysis

An analysis of variance (ANOVA) was conducted on the chloroplast ultrastructure data using IBM SPSS Statistics 26.0 software, followed by a Tukey's b-test for treatment comparisons (p = 0.05). ANOVA for the photosynthetic efficiency parameters was conducted using Tibco Statistica version 7. The Shapiro–Wilk normality test was used to test for the normality of the collected data. The Fischer's protected least significant differences (LSD) test at the alpha value of p = 0.05 was used for mean separation.

3. Results

3.1. Effects of Heat Stress on Photosynthetic Efficiency Parameters

Heat stress significantly impacted various photosynthetic efficiency parameters in the three edamame cultivars. The HS-I treatment had no significant effect on most photosynthetic efficiency parameters in both UVE17 and UVE14 either at the flowering or pod-filling stage. However, at the flowering stage, the HS-II treatment led to notable increases in chlorophyll a (56%), chlorophyll b (49%), and carotenoids (31%) in UVE17. Similarly, this treatment significantly increased the pigments chl-a (97% increase), chl-b (105% increase), and carotenoids (23% increase) in UVE14. Contrary, in AGS354, when exposed to HS-II, the cultivar showed a significant decrease in chl-a (43%), while chl-b and carotenoids remained stable (Table 1). At pod-filling under HS-II treatment, UVE17 showed a substantial increase (82%) for chl-a only, while chl-b and carotenoids remained unchanged. For UVE14, both chl-a and chl-b were substantially increased (113% and 72%, respectively) under HS-II treatment. The chl-a and chl-b remained unchanged under HS-II treatment in AGS354, while carotenoids were substantially reduced (27%). The only increase in photosynthetic pigments for this cultivar was under mild-temperature (HS-I) treatments (Table 2).

Table 1. The photosynthetic efficiency parameters of three edamame cultivars under heat stress at the flowering stage.

Treatment	Chl-a (mg/g fw)	Chl-b (mg/g fw)	CRDs (mg/g fw)	Fv/Fm (a.u)	PIabs (a.u)	PItot (a.u)	SC (mmol/m^2/s)	TSS (mg glucose/g fw)
UVE17 Control	8.820 ^{bcd}	7.650 ^{ab}	9.820 ^{b}	0.8330 ^{d}	9.377 ^{f}	7.288 ^{f}	160.0 ^{a}	0.221 ^{a}
UVE17 HS-I	8.550 ^{bc}	7.720 ^{ab}	11.03 ^{bc}	0.8202 ^{bcd}	5.182 ^{cd}	3.084 ^{bcd}	160.5 ^{a}	0.228 ^{a}
UVE17 HS-II	13.76 ^{e}	11.39 ^{bc}	12.96 ^{cd}	0.8149 ^{bc}	4.115 ^{bc}	1.875 ^{ab}	145.5 ^{a}	0.157 ^{a}
AGS354 Control	6.770 ^{ab}	5.290 ^{a}	7.51 ^{a}	0.8311 ^{cd}	5.705 ^{cde}	4.141 ^{cde}	179.3 ^{ab}	0.235 ^{a}
AGS354 HS-I	14.07 ^{e}	13.12 ^{c}	12.40 ^{c}	0.8166 ^{bcd}	2.273 ^{ab}	1.135 ^{ab}	255.6 ^{c}	0.287 ^{a}
AGS354 HS-II	3.880 ^{a}	3.670 ^{a}	6.71 ^{a}	0.7837 ^{a}	1.756 ^{a}	0.928 ^{a}	208.8 ^{abc}	0.195 ^{a}
UVE14 Control	12.68 ^{cde}	10.29 ^{bc}	12.05 ^{c}	0.8274 ^{cd}	6.820 ^{de}	5.741 ^{ef}	245.6 ^{bc}	0.182 ^{a}
UVE14 HS-I	12.97 ^{de}	9.990 ^{bc}	12.16 ^{c}	0.8230 ^{bcd}	7.385 ^{e}	4.347 ^{de}	338.5 ^{d}	0.223 ^{a}
UVE14 HS-II	25.07 ^{f}	21.11 ^{d}	14.79 ^{d}	0.8082 ^{b}	4.656 ^{c}	2.202 ^{abc}	341.2 ^{d}	0.235 ^{a}

Values represent means (n = 3). Different mean letters within the columns indicate significant differences between treatments ($p \leq 0.05$). Abbreviations: chl-a = chlorophyll a, chl-b = chlorophyll b, CRDs = carotenoids, fw: fresh weight, control = 25/18 °C, HS-I = 30/23 °C, HS-II = 35/28 °C.

The effects of heat stress on the efficiency of the light-dependent reactions of photosynthesis are also represented in Table 1. Although Fv/Fm was reduced under HS-II treatment in all cultivars at both reproductive stages, the highest reduction was observed at flowering in AGS354. During the flowering stage, HS-II treatment reduced the PIabs and PItot significantly in UVE17 (56% and 74% decrease, respectively), AGS354 (69% and 78%, respectively), and UVE14 (32% and 61% decrease, respectively). Similarly, at pod-filling, these parameters remained substantially reduced in UVE17 and UVE14 under HS-II treatment. In contrast, at the pod-filing stage, HS-II treatment was not significant for these parameters in AGS354 (Tables 1 and 2).

At flowering, the SC for UVE17 was not significantly affected by HS-II treatment. In contrast, the treatment increased SC significantly in UVE14 (1.4-fold increase) and AGS354 (1.2-fold increase). At pod-filling, however, all cultivars had reduced SC under HS-II treatment, with UVE14 showing the least reduction (Tables 1 and 2).

Table 2. The photosynthetic efficiency parameters of three edamame cultivars under heat stress at the pod-filling stage.

Treatment	Chl-a (mg/g fw)	Chl-b (mg/g fw)	CRDs (mg/g fw)	Fv/Fm (a.u)	PIabs (a.u)	PItot (a.u)	SC (mmol/m^2/s)	TSS (mg glucose/g fw)
UVE17 Control	12.69 ^{abc}	12.32 ^{bc}	14.11 ^{bc}	0.841 ^{d}	14.87 ^{e}	13.40 ^{d}	417.1 ^{c}	0.265 ^{c}
UVE17 HS-I	9.190 ^{a}	10.44 ^{a}	12.68 ^{bc}	0.8232 ^{bc}	9.114 ^{cd}	6.328 ^{bc}	115.7 ^{ab}	0.203 ^{ab}
UVE17 HS-II	23.15 ^{bc}	15.54 ^{bc}	13.64 ^{bc}	0.8149 ^{abc}	6.355 ^{abc}	3.737 ^{ab}	38.76 ^{a}	0.229 ^{bc}
AGS354 Control	12.92 ^{abc}	10.92 ^{a}	12.38 ^{b}	0.8208 ^{abc}	3.383 ^{a}	1.924 ^{a}	474.8 ^{c}	0.212 ^{b}
AGS354 HS-I	23.96 ^{bc}	18.65 ^{c}	13.90 ^{bc}	0.8181 ^{abc}	5.110 ^{ab}	2.921 ^{ab}	113.9 ^{ab}	0.160 ^{a}
AGS354 HS-II	12.93 ^{abc}	9.460 ^{a}	9.07 ^{a}	0.8088 ^{a}	4.553 ^{a}	1.985 ^{a}	60.28 ^{ab}	0.220 ^{bc}
UVE14 Control	11.71 ^{ab}	11.10 ^{a}	14.12 ^{bc}	0.8268 ^{c}	10.043 ^{d}	9.412 ^{c}	485.9 ^{c}	0.200 ^{ab}
UVE14 HS-I	16.23 ^{abc}	12.74 ^{bc}	15.57 ^{c}	0.8279 ^{cd}	7.925 ^{bcd}	5.841 ^{b}	116.9 ^{ab}	0.226 ^{bc}
UVE14 HS-II	24.97 ^{c}	19.12 ^{c}	15.34 ^{bc}	0.8103 ^{ab}	4.437 ^{a}	1.954 ^{a}	136.8 ^{b}	0.162 ^{a}

Values represent means (n = 3). Different mean letters within the columns indicate significant differences between treatments ($p \leq 0.05$). Abbreviations: chl-a = chlorophyll a, chl-b = chlorophyll b, CRDs = carotenoids, fw: fresh weight, control = 25/18 °C, HS-I = 30/23 °C, HS-II = 35/28 °C.

The HS-II treatment at both flowering and pod-filling stages did not have any significant effects on the TSS content for all cultivars (Tables 1 and 2).

3.2. Effects of Heat Stress on Chloroplast Ultrastructure

The effects of heat stress on photosynthesis were further examined at the ultrastructural level. Based on the above-measured photosynthetic efficiency parameters, carotenoid content at pod-filling was the only parameter with clear differences between the cultivars. Therefore, the micromorphological investigations were only conducted at the pod-filling stage. In cultivar AGS354, HS-II treatment led to a significant reduction in mesophyll cell size (MCS, 37% decrease) and total chloroplast area (TCA, 31% decrease) compared to the control. The average chloroplast area (ACA) was substantially reduced under HS-II (41% decrease), while the total number of chloroplasts per mesophyll cell (TNCPMC) was increased. The effects of heat on the grana characteristics were also studied in this cultivar. The highest impacts were observed under HS-II treatment where there were significant reductions in the total grana area (TGA, 40% decrease), average grana area (AGA, 42% decrease), grana height (GH, 58% decrease), and grana lamella/lumen thickness (GLT, 25% decrease). In contrast, the percent grana area (PGA) was significantly increased (89%) under HS-II treatment. Furthermore, the total grana number per chloroplast (TGNPC) was slightly increased under HS-II treatment. For the plastoglobule traits, only the total plastoglobule area (TPA) and percent plastoglobule area (PPA) were significantly reduced under HS-II treatment. The total number of plastoglobules per chloroplast (TNPPC) and average plastoglobule area (APA) were not sensitive to increased temperatures for this cultivar. All starch parameters were significantly increased under HSII treatment in AGS354 (Table 3, Figure 1).

Table 4 and Figure 2 show the effects of heat stress on the chloroplast ultrastructure characteristics of UVE14. Chloroplast characteristics such as TCA and ACA were not affected by either HS-I or HS-II treatments in UVE14, while MCS and TNCPMC were significantly reduced (1.7-fold decrease for each). For the grana traits, the HS-II treatment significantly increased TGA by 1.5-fold and PGA by 1.3-fold. Other grana traits were not significantly influenced by HS-II treatment. Compared to the HS-II treatment, fewer plastoglubule traits were affected under the HS-I treatment in this cultivar. Compared to

the control, TNPPC, TPA, and APA were not affected by HS-II treatment. Contrary, the PPA was significantly increased under HS-II treatment (117% increase). For this cultivar, the largest increases in starch traits were observed under the HS-II treatment, with significant increases in TNSGPC (3.2-fold increase), TSGA (6.1-fold increase), and PSGA (7.1-fold increase). The ASGA remained unaffected under HS-II treatment in this cultivar.

Table 3. Effects of heat stress on the chloroplast ultrastructure properties of edamame cultivar AGS354.

Micromorphological Traits	Control	HS-I	HS-II
Mesophyll cell size (MCS, μm^2)	149.9 ^{b}	91.88 ^{a}	94.94 ^{a}
Total number of chloroplasts per mesophyll cell (TNCPMC, No.)	5.000 ^{ab}	3.800 ^{a}	6.600 ^{b}
Total chloroplast area (TCA, μm^2)	98.88 ^{b}	43.93 ^{a}	68.17 ^{a}
Average chloroplast area (ACA, μm^2)	16.49 ^{b}	12.39 ^{ab}	9.670 ^{a}
Total grana number per chloroplast (TGNPC, No.)	27.14 ^{ab}	24.00 ^{a}	29.00 ^{b}
Total grana area (TGA, μm^2)	3.002 ^{c}	2.813 ^{b}	1.789 ^{a}
Average grana area (AGA, μm^2)	0.111 ^{b}	0.117 ^{b}	0.064 ^{a}
Percent grana area (PGA, %)	14.75 ^{a}	19.95 ^{b}	27.91 ^{c}
Grana height (GH, μm)	0.260 ^{b}	0.150 ^{ab}	0.110 ^{a}
Grana lamella/lumen thickness (GLT, μm)	0.016 ^{b}	0.014 ^{ab}	0.012 ^{a}
Total number of starch grains per chloroplast (TNSGPC, No.)	0.500 ^{a}	3.9000 ^{b}	2.910 ^{b}
Total starch grain area (TSGA, μm^2)	0.033 ^{a}	4.730 ^{b}	1.340 ^{ab}
Average starch grain area (ASGA, μm^2)	0.033 ^{a}	1.470 ^{b}	0.360 ^{ab}
Percent starch grain area (PSGA, %)	0.210 ^{a}	13.06 ^{b}	5.730 ^{ab}
Total number of plastoglobules per chloroplast (TNPPC, No.)	12.00 ^{a}	12.00 ^{a}	14.40 ^{a}
Total plastoglobule area (TPA, μm^2)	0.195 ^{c}	0.025 ^{a}	0.067 ^{b}
Average plastoglobule area (APA, μm^2)	0.012 ^{a}	0.002 ^{a}	0.004 ^{a}
Percent plastoglobule area (PPA, %)	2.110 ^{c}	0.362 ^{a}	1.010 ^{b}

Data represent means (n = 10). Means within the lines followed by the same letter are not statistically significant at $p \leq 0.05$. Control = 25/18 °C, HS-I = 30/23 °C, HS-II = 35/28 °C.

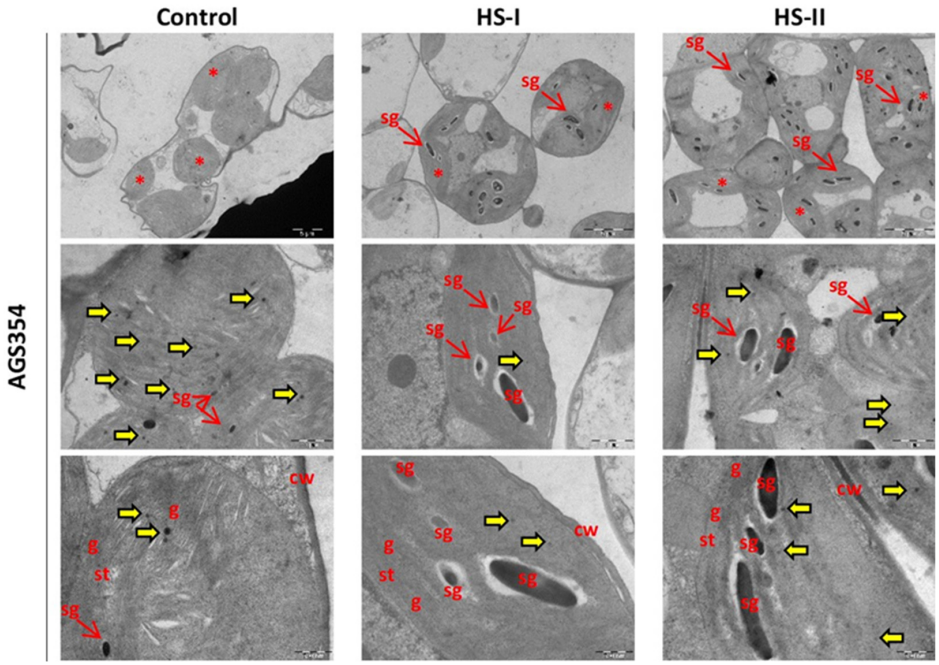

Figure 1. Chloroplast ultrastructure of heat-stress-treated edamame cultivar AGS354. The images shown here are in three magnifications (6000× for complete mesophyll cell, 8000× and 11,500× for complete chloroplast, and 66,000× for grana). The scale bar for each image shows 5 μm for the 6000× magnification, 2 μm for the 8000× magnification, 1 μm for the 11,500× magnification, and 0.2 μm for the 66,000× magnification. Control = 25/18 °C, HS-I = 30/23 °C, HS-II = 35/28 °C. g: grana, st: stromal thylakoid, sg: starch grain, cw: cell wall. Chloroplast is identified with *. Yellow arrows mark plastoglobules.

Table 4. Effects of heat stress on the chloroplast ultrastructure properties of edamame cultivar UVE14.

Micromorphological Traits	Control	HS-I	HS-II
Mesophyll cell size (MCS, μm^2)	191.1 ^{b}	116.8 ^{a}	113.3 ^{a}
Total number of chloroplasts per mesophyll cell (TNCPMC, No.)	7.570 ^{b}	5.200 ^{ab}	4.550 ^{a}
Total chloroplast area (TCA, μm^2)	111.4 ^{a}	63.17 ^{a}	84.73 ^{a}
Average chloroplast area (ACA, μm^2)	14.18 ^{a}	14.07 ^{a}	13.62 ^{a}
Total grana number per chloroplast (TGNPC, No.)	50.00 ^{a}	45.00 ^{a}	79.00 ^{a}
Total grana area (TGA, μm^2)	2.082 ^{a}	2.458 ^{b}	3.195 ^{c}
Average grana area (AGA, μm^2)	0.042 ^{a}	0.055 ^{b}	0.040 ^{a}
Percent grana area (PGA, %)	18.14 ^{a}	27.96 ^{c}	24.61 ^{b}
Grana height (GH, μm)	0.130 ^{a}	0.150 ^{a}	0.160 ^{a}
Grana lamella/lumen thickness (GLT, μm)	0.011 ^{a}	0.013 ^{b}	0.012 ^{ab}
Total number of starch grains per chloroplast (TNSGPC, No.)	1.200 ^{a}	1.800 ^{a}	3.820 ^{b}
Total starch grain area (TSGA, μm^2)	0.080 ^{a}	0.160 ^{a}	0.490 ^{b}
Average starch grain area (ASGA, μm^2)	0.060 ^{a}	0.110 ^{a}	0.140 ^{a}
Percent starch grain area (PSGA, %)	0.550 ^{a}	1.420 ^{a}	3.870 ^{b}
Total number of plastoglobules per chloroplast (TNPPC, No.)	9.400 ^{b}	5.160 ^{a}	9.000 ^{b}
Total plastoglobule area (TPA, μm^2)	0.061 ^{b}	0.025 ^{a}	0.064 ^{b}
Average plastoglobule area (APA, μm^2)	0.008 ^{a}	0.002 ^{a}	0.007 ^{a}
Percent plastoglobule area (PPA, %)	0.361 ^{b}	0.318 ^{a}	0.785 ^{c}

Data represent means (n = 10). Means within the lines followed by the same letter are not statistically significant at $p \leq 0.05$. Control = 25/18 °C, HS-I = 30/23 °C, HS-II = 35/28 °C.

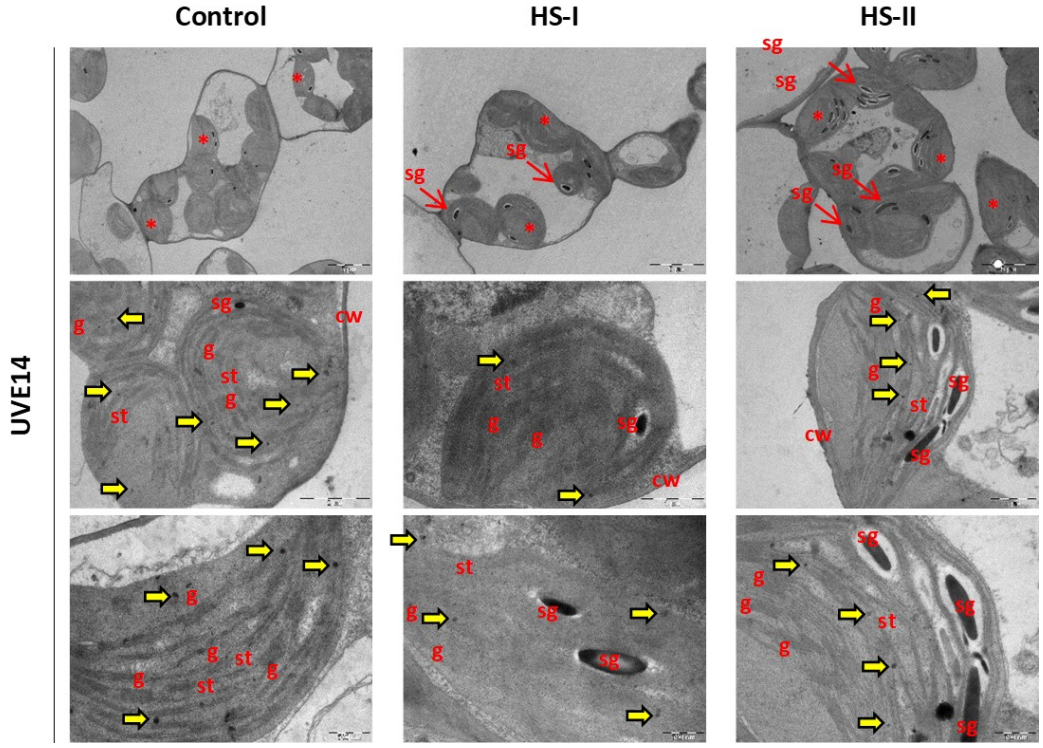

Figure 2. Chloroplast ultrastructure of heat-stress-treated edamame cultivar UVE14. The images are shown in three magnifications (6000× for complete mesophyll cell, 8000× and 11,500× for complete chloroplast, and 66,000× for grana). The scale bar for each image shows 5 μm for the 6000× magnification, 2 μm for the 8000 magnification, 1 μm for the 11,500× magnification, and 0.2 μm for the 66,000× magnification. Control = 25/18 °C, HS-I = 30/23 °C, HS-II = 35/28 °C. g: grana, st: stromal thylakoid, sg: starch grain, cw: cell wall. Chloroplast is identified with *. Yellow arrows mark plastoglobules.

Table 5 and Figure 3 present the chloroplast ultrastructure traits of UVE17 under high-temperature stress treatments. The HS-II treatment had no significant effect on the MCS, TNCPMC, TCA, and ACA for this cultivar. Similarly, grana traits such as TGNPC, GH,

and GLT were unaffected by HS-II treatment. Grana characteristics that were significantly increased under this treatment included TGA (2.6-fold increase), AGA 2.4-fold increase), and PGA (1.3-fold increase). For the plastoglobule traits, HS-II treatment had no significant effect on APA. Furthermore, this treatment reduced PPA (27% decrease) and increased TNPPC and TPA by 90 and 44%, respectively.

Table 5. Effects of heat stress on the chloroplast ultrastructure properties of edamame cultivar UVE17.

Micromorphological Traits	Control	HS-I	HS-II
Mesophyll cell size (MCS, μm^2)	116.8 ^{a}	113.42 ^{a}	141.6 ^{a}
Total number of chloroplasts per mesophyll cell (TNCPMC, No.)	7.710 ^{b}	4.900 ^{a}	7.710 ^{b}
Total chloroplast area (TCA, μm^2)	93.54 ^{a}	57.52 ^{a}	82.59 ^{a}
Average chloroplast area (ACA, μm^2)	9.030 ^{a}	13.07 ^{a}	11.95 ^{a}
Total grana number per chloroplast (TGNPC, No.)	32.00 ^{a}	40.00 ^{b}	35.00 ^{a}
Total grana area (TGA, μm^2)	1.266 ^{a}	2.173 ^{b}	3.229 ^{c}
Average grana area (AGA, μm^2)	0.039 ^{a}	0.054 ^{b}	0.092 ^{c}
Percent grana area (PGA, %)	19.66 ^{a}	18.83 ^{b}	24.99 ^{c}
Grana height (GH, μm)	0.180 ^{a}	0.150 ^{a}	0.190 ^{a}
Grana lamella/lumen thickness (GLT, μm)	0.011 ^{b}	0.009 ^{a}	0.012 ^{b}
Total number of starch grains per chloroplast (TNSGPC, No.)	0.400 ^{a}	1.400 ^{a}	3.090 ^{b}
Total starch grain area (TSGA, μm^2)	0.028 ^{a}	0.385 ^{b}	0.452 ^{b}
Average starch grain area (ASGA, μm^2)	0.028 ^{a}	0.197 ^{b}	0.191 ^{b}
Percent starch grain area (PSGA, %)	0.130 ^{a}	2.820 ^{b}	3.33 ^{b}
Total number of plastoglobules per chloroplast (TNPPC, No.)	5.550 ^{a}	7.300 ^{a}	10.60 ^{b}
Total plastoglobule area (TPA, μm^2)	0.043 ^{b}	0.029 ^{a}	0.062 ^{c}
Average plastoglobule area (APA, μm^2)	0.005 ^{a}	0.004 ^{a}	0.005 ^{a}
Percent plastoglobule area (PPA, %)	0.824 ^{c}	0.251 ^{a}	0.605 ^{b}

Data represent means (n = 10). Means within the lines followed by the same letter are not statistically significant at $p \leq 0.05$. Control = 25/18 °C, HS-I = 30/23 °C, HS-II = 35/28 °C.

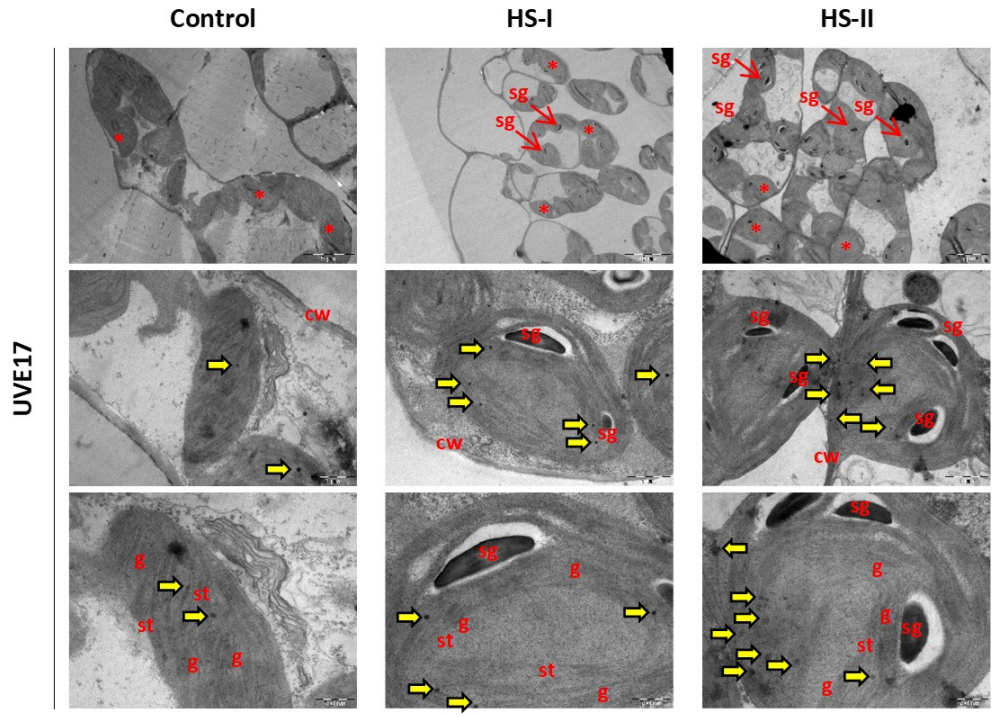

Figure 3. Chloroplast ultrastructure of heat-stress-treated edamame cultivar UVE17. The images are shown in three magnifications (6000× for complete mesophyll cell, 8000× and 11,500× for complete chloroplast, and 66,000× for grana). The scale bar for each image shows 5 μm for the 6000× magnification, 2 μm for the 8000 magnification, 1 μm for the 11,500× magnification, and 0.2 μm for the 66,000× magnification. Control = 25/18 °C, HS-I = 30/23 °C, HS-II = 35/28 °C. g: grana, st: stromal thylakoid, sg: starch grain, cw: cell wall. Chloroplast is identified with *. Yellow arrows mark plastoglobules.

The HS-II treatment led to substantial increases in TNSGPC (7.7-fold), TSGA (16.1-fold), ASGA (6.8-fold), and PSGA (25.6-fold).

The performance comparison of micromorphological traits across cultivars is presented in Table 6. Under HS-II treatment, cultivars showed no significant differences in MCS, TCA, ACA, GLT, TNSGPC, PSGA, TPA, and APA. AGS354 had the lowest TGNPC, TGA, and GH, but recorded the highest PGA, TSGA, ASGA, TNPPC, and PPA. UVE17 recorded the highest TNCPMC and AGA, while UVE14 had the highest TGNPC. Both UVE14 and UVE17 showed similarly high performance for TGA (Table 6).

Table 6. A comparison of micromorphological traits among edamame cultivars subjected to the HS-II treatment during the pod-filling stage.

HS-II	AGS354	UVE14	UVE17
Mesophyll cell size (MCS, μm^2)	94.94 ^{a}	113.3 ^{a}	141.6 ^{a}
Total number of chloroplasts per mesophyll cell (TNCPMC, No.)	6.600 ^{ab}	4.550 ^{a}	7.710 ^{b}
Total chloroplast area (TCA, μm^2)	68.17 ^{a}	84.73 ^{a}	82.59 ^{a}
Average chloroplast area (ACA, μm^2)	9.670 ^{a}	13.62 ^{a}	11.95 ^{a}
Total grana number per chloroplast (TGNPC, No.)	29.00 ^{a}	79.00 ^{c}	35.00 ^{b}
Total grana area (TGA, μm^2)	1.789 ^{a}	3.195 ^{b}	3.229 ^{b}
Average grana area (AGA, μm^2)	0.064 ^{b}	0.040 ^{a}	0.092 ^{c}
Percent grana area (PGA, %)	27.91 ^{b}	24.61 ^{a}	24.99 ^{a}
Grana height (GH, μm)	0.110 ^{a}	0.160 ^{ab}	0.190 ^{b}
Grana lamella/lumen thickness (GLT, μm)	0.012 ^{a}	0.012 ^{a}	0.012 ^{a}
Total number of starch grains per chloroplast (TNSGPC, No.)	2.910 ^{a}	3.820 ^{a}	3.090 ^{a}
Total starch grain area (TSGA, μm^2)	1.340 ^{b}	0.490 ^{a}	0.452 ^{a}
Average starch grain area (ASGA, μm^2)	0.360 ^{b}	0.140 ^{a}	0.191 ^{a}
Percent starch grain area (PSGA, %)	5.730 ^{a}	3.870 ^{a}	3.330 ^{a}
Total number of plastoglobules per chloroplast (TNPPC, No.)	14.40 ^{b}	9.000 ^{a}	10.06 ^{a}
Total plastoglobule area (TPA, μm^2)	0.067 ^{a}	0.064 ^{a}	0.062 ^{a}
Average plastoglobule area (APA, μm^2)	0.004 ^{a}	0.007 ^{a}	0.005 ^{a}
Percent plastoglobule area (PPA, %)	1.010 ^{c}	0.785 ^{b}	0.605 ^{a}

Values represent means (n = 10). Means within the lines followed by the same letter are not statistically significant at $p \leq 0.05$. HS-II = 35/28 °C.

4. Discussion

The discussion focuses on photosynthetic responses under the highest temperature treatment (HS-II, 35/28 °C), which had the greatest impact on most traits and cultivars studied. Photosynthetic pigments are essential components of the photosynthesis process [31]. Although not significant, the reduction in the chlorophyll (chl)-a level in cultivar AGS354 under HS-II treatment at the flowering stage corresponds to a reduced maximum quantum efficiency of photosystem (PS) II (Fv/Fm). This suggests that under HS-II, photosynthetic pigments did not effectively capture light, leading to less energy absorbed for the photochemical reactions in PSII, adversely impacting the electron transport in PSII. Although the efficiency of PSII was negatively affected compared to the control, the overall efficiency of the light-dependent reactions (PItot) was not affected at pod-filling, showing the damage caused by heat in AGS354 targeted PSII. A similar response was observed in soybeans under heat stress, where a reduction in Fv/Fm did not affect net photosynthesis [13]. In agreement, Ergo et al. [22] further showed that heat stress in soybeans damaged PSII, resulting in reduced photosynthesis. They further demonstrated a strong correlation between improved Fv/Fm, chlorophyll content, and yield under heat stress, suggesting that the compromised PSII in heat-stressed AGS354 may lead to increased non-photochemical quenching [12]. Notably, this was the only cultivar to exhibit reduced carotenoid accumulation under the HS-II treatment. This suggests greater susceptibility to heat stress,

as carotenoids play a crucial role in photoprotection, safeguarding the photosynthetic apparatus, and providing antioxidative defence [32].

Moreover, HS-II treatment significantly increased stomatal conductance (SC) at the flowering stage in AGS354, suggesting improved CO_2 fixation by Rubisco and greater accumulation of photoassimilates [33]. However, there was no significant increase in total soluble sugar (TSS) production in this cultivar at the flowering stage, despite the potential for high CO_2 fixation under heat stress. This aligns with the findings of Zhang et al. [34], who also reported no increase in TSS levels during heat stress, despite high CO_2 fixation rates. Jumrani et al. [12] and Ergo et al. [22] showed that changes at structural level were responsible for reduced photosynthesis in heat-stressed soybeans.

The impact of heat treatment on chloroplast ultrastructure was explored for this cultivar at the pod-filling stage. The HS-II treatment increased all the micromorphological traits associated with the starch grains in AGS354, explaining the observed insignificant or little accumulation in TSS in this cultivar. This suggests that HS-II treatment in AGS354 alters carbohydrate metabolism, favouring starch storage over the assimilation of simple sugars. Compared to UVE14 and UVE17, AGS354 had the highest TSGA and ASGA. The excessive accumulation of starch grains in AGS354 suggests a high vulnerability to heat stress, as large starch grains may distort thylakoid membranes [35], potentially disrupting the electron transport chain and impairing PSII functionality.

Since photosynthesis occurs in the mesophyll cell's chloroplasts, the reduced mesophyll cell size (MCS) under HS-II treatment could be an indication that the cultivar's photosynthetic capacity is negatively affected because, for vascular plants, increased mesophyll area represents high CO_2 diffusion [36]. Xiong et al. [37] showed that increased chloroplast surface area leads to high photosynthesis while large chloroplast size impairs photosynthesis. Glowacka et al. [38] also showed that increased chloroplast size in tobacco reduced chloroplast movement and non-photochemical quenching, leading to reduced photosynthesis. Therefore, the significant reduction in the mesophyll cell size (MCS), total chloroplast area (TCA), and average chloroplast area (ACA) observed in heat-stressed AGS354 further highlights the detrimental effects of heat stress on this cultivar. A reduction in these characteristics corresponds to reduced chl-a accumulation in this cultivar. Heat stress can alter the arrangement and division of chloroplasts, leading to a reduction in their size [15]. Previous studies, such as those by Paul et al. [39] and Wang et al. [40], have reported a decrease in chloroplast size linked to chlorophyll degradation under heat stress.

Heat stress also results in a reduction in grana size [41,42], which is linked to damage to the photosynthetic apparatus and the destabilisation of membrane structures. Over time, these processes lead to grana disassembly and the destruction of thylakoid membranes [43]. Additionally, heat stress increases the reactive oxygen species (ROS) production in chloroplasts, causing oxidative stress, which further contributes to the degradation of thylakoid membranes and a reduction in granum size [44]. The reduced grana characteristics [total grana area (TGA), average grana area (AGA), grana height (GH), and grana lamella/lumen area (GLA)] further demonstrate the negative impact of heat stress on AGS354. Since the grana comprise a stack of thylakoids, which are important sites for chlorophyll synthesis and electron transport during light-dependent reactions, any negative impact on them could also explain the reduced chl-a content in this cultivar. In soybeans, it was found that the disruption of the vesicular structure of thylakoid membranes decreased the thermal stability of PSII [45], further supporting the suggestion that photosynthesis was not efficient in AGS354 under heat stress. Smaller grana promote more efficient linear electron transport, while larger grana enhance cyclic electron transfer [46]. The reduced GH in AGS354 suggests increased linear electron transport during heat stress. However, this does not yield positive results, as heat stress impairs PSII in this cultivar, reducing the availability

of electrons to initiate the transport chain. Reduced carotenoid content in HS-II-treated AGS354 likely contributes to oxidative stress, impacting the structural integrity of the grana. This disruption negatively affects the photosynthetic machinery, contributing to the observed reduced photosynthesis. Based on the grana traits, AGS354 was the most vulnerable cultivar under HS-II stress. It exhibited the lowest grana trait values, which corresponded to a significantly reduced photosynthetic efficiency.

Plastoglobules are another micromorphological character explaining how AGS354 responded to increased temperature treatment. The reduction in total plastoglobule area (TPA) and percentage of plastoglobule area (PPA) further shows that HS-II treatment reduced the photosynthesis in this cultivar. This reduction may be linked to heat-induced oxidative stress, which oxidises lipids in plastoglobules, causing their shrinkage and depleting energy reserves. This limits the plant's capacity to respond to stress and maintain cellular functions [21]. In contrast, Carrera et al. [15] showed that in soybeans, heat stress increased plastoglobules accumulation. The reduced plastoglobule area in AGS354 corresponds to reduced carotenoids at pod-filling, further suggesting poor photosynthesis in this cultivar under heat stress.

Cultivar UVE17 responded to heat stress through improved light-absorption capacity, with increased chl-a (at both reproductive stages) and chl-b (only at pod-filling). This shows that under HS-II, enough energy was available to initiate the electron transport in PSII. Increased carotenoid content at flowering corresponds to increased chl-a, showing that this cultivar has a high capacity of protecting chlorophyll and PSII from oxidation under heat stress. Despite sufficient energy being available, the Fv/Fm and performance indices, PIabs and PItot, were reduced, indicating that the problem during heat stress lies beyond the light-harvesting capability of this cultivar. This suggests that heat stress impairs the light-dependent electron transport chain, with a possible increase in non-photochemical quenching, reducing the photochemical reactions [47]. Furthermore, in UVE17, HS-II treatment reduced SC at pod-filling, implying that there was insufficient CO_2 substrate available to initiate the Calvin cycle. However, this fixation may be affected negatively because of the reduced efficiency of the light-dependent reactions (the cultivar had reduced photochemical reactions), which supply NADPH and ATP for the reduction and regeneration steps of the Calvin cycle [48], further reducing photosynthesis in this cultivar. Despite the enhanced light-harvesting capacity and increased carotenoid levels in this cultivar, both the light-dependent and light-independent reactions were adversely affected. This indicates that while carotenoids play a significant role in mitigating heat stress, they alone are insufficient to fully counteract the decline in photosynthesis. Increased grana area traits (TGA, AGA, and PGA) correspond to the observed strong light-harvesting ability of this cultivar under heat stress. This enhancement in grana area properties may be attributed to the protective role of elevated carotenoid levels, which are essential for maintaining proper thylakoid stacking and membrane dynamics [49].

The increase in the plastoglobule traits (TNPPC and TPA) and starch grains (TNSGPC, TSGA, ASGA, and PSGA) under heat stress shows that this cultivar stores more energy reserves during heat stress, partly explaining why the TSS did not increase despite high SC. Since plastoglobules are associated with alterations in carotenoid storage and contribute to carotenoid accumulation and storage [50], the observed increase in TNPPC and TPA could be associated with the observed increase in the carotenoids for UVE17 under heat stress.

Cultivar UVE14 responded positively to HS-II treatment, with significantly increased chl-a and chl-b levels at the flowering stage. The treatment also enhanced carotenoid accumulation at both reproductive stages, demonstrating the cultivar's adaptation to heat stress through improved light-harvesting capacity and protection of the photosynthetic apparatus. Similar to UVE17, the HS-II treatment negatively impacted the photochemical reactions in

UVE14, as evidenced by reduced Fv/Fm, PIabs, and PItot. Although SC increased significantly at the flowering stage under HS-II treatment, the carbon fixation process may have been limited by the probable reduction in the photochemical reaction products, namely NADPH and ATP. This was accompanied by reduced accumulation of soluble sugars and increased starch grain area traits, indicating that the cultivar prioritised energy storage during heat stress. Notably, starch grain parameters in UVE14 remained the lowest among the cultivars, potentially minimising mechanical damage to the thylakoid membranes. Consistent with this, Du et al. [51] associated increased starch accumulation with heat stress tolerance in soybeans, explaining that starch acts as a temporary carbohydrate reserve that can be converted into sucrose for translocation to sink tissues, such as seeds. There, sucrose is broken down into hexoses, providing the substrates and energy required for pod growth and filling. Although mesophyll size and the number of chloroplasts decreased under HS-II treatment in UVE14, the traits associated with grana structure were not significantly influenced by heat stress. This corresponds to the increased chl-a and chl-b content in this cultivar under HS-II treatment. The plastoglobule numbers and size were not significantly affected under HS-II, except for the increased PPA. The increased or stabilised carotenoid accumulation under heat stress in UVE14 could be associated with the increased PPA and stable plastoglobule traits, which contributes to the stability of the thylakoid membranes, leading to improved grana stacking.

5. Conclusions

This study shows that the three edamame cultivars responded differently to heat stress, with the highest temperature (35/28 °C) having the most significant impact on the photosynthetic parameters of UVE17 and UVE14. Of all the cultivars, AGS354 was the most susceptible cultivar to heat stress with the highest reduction in the carotenoids, which account for the reduced chl-a production and reduced grana traits. Heat stress in this cultivar reduced plastoglobule traits (PPA and TPA), likely due to decreased carotenoid levels. The lack of carotenoids may also have contributed to the reduction in grana traits and chlorophyll content. While UVE14 and UVE17 improved their light-harvesting capability, their responses differed. UVE14 increased both chl-a and chl-b at both growth stages, whereas UVE17 did not increase chl-b at pod-filling. Despite these pigment increases, neither cultivar efficiently converted harvested light energy into chemical energy, highlighting that increased pigment accumulation does not necessarily enhance photosynthesis in this cultivar. The elevated carotenoid levels likely protected chlorophyll from degradation, preventing photo-oxidation caused by heat stress. Additionally, increased TGA, AGA, and PGA suggest that carotenoids contribute to grana protection, supporting the observed increase in chlorophyll. Since plastoglobules are involved in carotenoid biosynthesis, the increase or stabilisation of most plastoglobule traits in UVE14 and UVE17 under heat stress contributes to improved heat stress tolerance. Although carotenoid levels increase during heat stress as an adaptive response, they could not fully prevent the decline in photochemical reactions in edamame. This suggests that their primary role during heat stress tolerance is likely in the antioxidative mechanisms. Future studies should investigate additional ROS scavenging mechanisms that could complement carotenoids in enhancing heat stress tolerance in edamame. This study provides valuable insights for targeted heat tolerance breeding, suggesting UVE14 and UVE17 as potential candidates for such programs. Continued research into the physiological and molecular mechanisms underlying these responses will be essential for developing effective strategies to sustain edamame production under rising global temperatures. Although this study adds value, field studies are crucial to confirm these findings and adapt them to practical agricultural applications.

Author Contributions: Conceptualisation, M.J.M.; methodology, M.J.M. and C.T.; validation, C.T. and B.T.; formal analysis, M.J.M. and C.T.; investigation, A.H.; resources, M.J.M. and B.T.; data curation, A.H.; writing—original draft preparation, M.J.M.; writing—review and editing, C.T. and B.T.; visualisation, M.J.M. and C.T.; supervision, M.J.M.; project administration, M.J.M.; funding acquisition, M.J.M. All authors have read and agreed to the published version of the manuscript.

Funding: This research was funded by the National Research Foundation, South Africa (Reference: TTK210329591284).

Data Availability Statement: All data are included in the article.

Acknowledgments: We thank Lize Henning and the Department of Soil, Crop, and Climate Sciences for access to the walk-in climate chambers. We also extend our gratitude to Rouxlene van der Merwe and the Edamame Development Program (EDP) for supplying the seed material. Additionally, we thank the Centre for Microscopy at the University of the Free State for preparing the samples for TEM.

Conflicts of Interest: The authors declare no conflicts of interest. The funder had no role in the project or in the decision to publish the results.

References

1. Djanta, M.K.A.; Agoyi, E.E.; Agbahoungba, S.; Quenum, F.J.-B.; Chadare, F.J.; Assogbadjo, A.E.; Agbangla, C.; Sinsin, B. Vegetable soybean, edamame: Research, production, utilization and analysis of its adoption in Sub-Saharan Africa. *J. Hortic. For.* **2020**, *12*, 1–12. [CrossRef]
2. Jiang, G.L.; Mireku, P.; Johnson, D.; Townsend, W.; Seow, A.; Fallen, B.; Carter, T. Evaluation of 10 Edamame Breeding Lines to Determine Yield, Agronomic, and Seed Composition Traits. *HortScience* **2024**, *59*, 1789–1794. [CrossRef]
3. Shurtleff, W.; Aoyagi, A. *History of Soybeans and Soyfoods in South America (1884–2009): Extensively Annotated Bibliography and Sourcebook*; Soyinfo Center: Lafayette, CA, USA, 2009.
4. El Zein, A.; Chehayeb, N. The effect of greenhouse gases on earth's temperature. *Int. J. Environ. Monit. Anal.* **2015**, *3*, 74–79. [CrossRef]
5. Rowlands, D.J.; Rowlands, D.J.; Frame, D.J.; Ackerley, D.; Ackerley, D.; Aina, T.; Booth, B.B.; Christensen, C.; Collins, M.; Faull, N.; et al. Broad range of 2050 warming from an observationally constrained large climate model ensemble. *Nat. Geosci.* **2012**, *5*, 256–260. [CrossRef]
6. Pielke, R., Jr.; Burgess, M.G.; Ritchie, J. Plausible 2005–2050 emissions scenarios project between 2 °C and 3 °C of warming by 2100. *Environ. Res. Lett.* **2022**, *17*, 024027. [CrossRef]
7. Lobell, D.B.; Asner, G.P. Climate and management contributions to recent trends in US agricultural yields. *Science* **2003**, *299*, 1032. [CrossRef]
8. Schrader, S.M.; Kleinbeck, K.R.; Sharkey, T.D. Rapid heating of intact leaves reveals initial effects of stromal oxidation on photosynthesis. *Plant Cell Environ.* **2007**, *30*, 671–678. [CrossRef]
9. Wahid, A.; Gelani, S.; Ashraf, M.; Foolad, M. Heat tolerance in plants: An overview. *Environ. Exp. Bot.* **2007**, *61*, 199–223. [CrossRef]
10. Johnson, M.P. Photosynthesis. *Essays Biochem.* **2016**, *60*, 255–273. [CrossRef]
11. Djanaguiraman, M.; Prasad, P.V.; Boyle, D.; Schapaugh, W. High-temperature stress and soybean leaves: Leaf anatomy and photosynthesis. *Crops Sci.* **2011**, *51*, 2125–2131. [CrossRef]
12. Jumrani, K.; Bhatia, V.; Pandey, G. Impact of elevated temperatures on specific leaf weight, stomatal density, photosynthesis and chlorophyll fluorescence in soybean. *Photosynth. Res.* **2017**, *131*, 333–350. [CrossRef] [PubMed]
13. Herritt, M.; Fritschi, F. Characterization of Photosynthetic Phenotypes and Chloroplast Ultrastructural Changes of Soybean (*Glycine max*) in Response to Elevated Air Temperatures. *Front. Plant Sci.* **2020**, *11*, 153. [CrossRef] [PubMed]
14. Yamamoto, Y.; Aminaka, R.; Yoshioka, M.; Khatoon, M.; Komayama, K.; Takenaka, D.; Yamashita, A.; Nijo, N.; Inagawa, K.; Morita, N.; et al. Quality control of photosystem II: Impact of light and heat stresses. *Photosynth. Res.* **2008**, *98*, 589–608. [CrossRef] [PubMed]
15. Carrera, C.; Solís, S.; Ferrucci, M.; Vega, C.; Galati, B.; Ergo, V.; Andrade, F.; Lascano, R. Leaf structure and ultrastructure changes induced by heat stress and drought during seed filling in field-grown soybean and their relationship with grain yield. *An. Acad. Bras. Cienc.* **2021**, *93*, e20191388. [CrossRef]
16. Xu, S.; Li, J.L.; Zhang, X.Q.; Wei, H.; Cui, L.J. Effects of heat acclimation pretreatment on changes of membrane lipid peroxidation, antioxidant metabolites, and ultrastructure of chloroplasts in two cool-season turfgrass species under heat stress. *Environ. Exp. Bot.* **2006**, *56*, 274–285. [CrossRef]

17. Peng, Q.; Zhou, Q. Influence of lanthanum on chloroplast ultrastructure of soybean leaves under ultraviolet-B stress. *J. Rare Earths* **2009**, *27*, 304–307. [CrossRef]
18. Bréhélin, T.K.; Kessler, F. The Plastoglobule: A Bag Full of Lipid Biochemistry Tricks. *Photochem. Photobiol.* **2008**, *84*, 1388–1394. [CrossRef]
19. Austin, J.R.; Frost, E.; Vidi, P.A.; Kessler, F.; Staehelina, L.A. Plastoglobules Are Lipoprotein Subcompartments of the Chloroplast That Are Permanently Coupled to Thylakoid Membranes and Contain Biosynthetic Enzymes. *Plant Cell* **2006**, *18*, 1693–1703. [CrossRef]
20. Kessler, F.; Vidi, P.A. Plastoglobule Lipid Bodies: Their Functions in Chloroplasts and their Potential for Applications. *Adv. Biochem. Engin/Biotechnol.* **2007**, *107*, 153–172. [CrossRef]
21. Zhang, R.; Wise, R.R.; Struck, K.R.; Sharkey, T.D. Moderate heat stress of Arabidopsis thaliana leaves causes chloroplast swelling and plastoglobule formation. *Photosynth. Res.* **2010**, *105*, 123–134. [CrossRef]
22. Ergo, V.; Lascano, R.; Vega, C.; Parola, R.; Carrera, C. Heat and water stressed field-grown soybean: A multivariate study on the relationship between physiological-biochemical traits and yield. *Environ. Exp. Bot.* **2018**, *148*, 1–11. [CrossRef]
23. Moloi, M.J.; Van der Merwe, R. Drought tolerance responses in vegetable-type soybean involve a network of biochemical mechanisms at flowering and pod-filling stages. *Plants* **2021**, *10*, 1502. [CrossRef] [PubMed]
24. Hlahla, J.M.; Mafa, M.S.; van der Merwe, R.; Moloi, M.J. Exploring edamame survival mechanisms under combined drought and heat stress: Photosynthesis efficiency and carbohydrate accumulation. *Plant Stress* **2024**, *14*, 100616. [CrossRef]
25. Van der Merwe, R.; Tyawana, S.; Van der Merwe, J.; Mwenye, O. Evaluation of drought tolerance indices in vegetable-type soybean. *Mol. Soc. Cient. Gal* **2018**, *18*, 19–31.
26. Grain, S.A. Growing Soybeans. 2019. Available online: https://www.grainsa.co.za/growing-soybeans-a-great-source-of-food,-protein-and-oil#:~:text=Ideally%20temperatures%20should%20be%20at,norms%20of%2025%C2%B0C.&text=Good%20yields%20are%20achieved%20in,prolifically%20and%20produce%20excessive%20foliage (accessed on 12 January 2024).
27. Stratonovitch, P.; Semenov, M.A. Heat tolerance around flowering in wheat identified as a key trait for increased yield potential in Europe under climate change. *J. Exp. Bot.* **2015**, *66*, 3599–3609. [CrossRef]
28. Spurr, A.R. A low viscosity epoxy resin embedding medium for electron microscopy. *J. Ultrastruct. Res.* **1969**, *26*, 31–43. [CrossRef]
29. Pareek, A.; Buyer, J.S.; Sharma, S.K.; Schütz, L.; Mathimaran, N.; Singla-Pareek, S.L.; Grossman, J.M.; Bagyaraj, D.J. Deciphering the Role of Trehalose in Tripartite Symbiosis Among Rhizobia, Arbuscular Mycorrhizal Fungi, and Legumes for Enhancing Abiotic Stress Tolerance in Crop Plants. *Front. Microbiol.* **2020**, *11*, 509919. [CrossRef]
30. Irigoyen, J.J.; Einerich, D.W.; Sánchez-Díaz, M. Water stress-induced changes in concentrations of proline and total soluble sugars in nodulated alfalfa (*Medicago sativa*) plants. *Physiol. Plant* **1992**, *84*, 55–60. [CrossRef]
31. Simkin, A.J.; Kapoor, L.; Doss, C.G.P.; Hofmann, T.A.; Lawson, T.; Ramamoorthy, S. The role of photosynthesis related pigments in light harvesting, photoprotection and enhancement of photosynthetic yield in planta. *Photosynth. Res.* **2022**, *152*, 23–42. [CrossRef]
32. Kim, S.; Lee, C.; Park, S.; Lim, Y.; Park, W.; Kim, H.; Ahn, M.; Kwak, S.; Kim, H. Overexpression of the Golden SNP-Carrying Orange Gene Enhances Carotenoid Accumulation and Heat Stress Tolerance in Sweetpotato Plants. *Antioxidants* **2021**, *10*, 51. [CrossRef]
33. Gu, Q.; Zhao, L.; Li, C.; Ren, J.; Zhang, J. Photochemical efficiency of photosystem II in inverted leaves of soybean [*Glycine max* (L.) Merr.] affected by elevated temperature and high light. *Front. Plant Sci.* **2022**, *12*, 772644. [CrossRef]
34. Zhang, Y.; Liu, X.; Wang, J. Effects of heat stress on total soluble sugars and starch accumulation in plants during reproductive stages. *J. Plant Physiol.* **2021**, *258*, 153–162.
35. Chinnusamy, V.; Khanna-Chopra, R. Effect of heat stress on grain starch content in diploid, tetraploid and hexaploid wheat species. *J. Agron. Crop Sci.* **2003**, *189*, 242–249. [CrossRef]
36. Théroux-Rancourt, G.; Roddy, A.; Earles, J.; Gilbert, M.; Zwieniecki, M.; Boyce, C.; Tholen, D.; McElrone, A.; Simonin, K.; Brodersen, C. Maximum CO_2 diffusion inside leaves is limited by the scaling of cell size and genome size. *Proc. R. Soc. B Biol. Sci.* **2021**, *288*, 20203145. [CrossRef]
37. Xiong, D.; Huang, J.; Peng, S.; Li, Y. A few enlarged chloroplasts are less efficient in photosynthesis than a large population of small chloroplasts in Arabidopsis thaliana. *Sci. Rep.* **2017**, *7*, 5782. [CrossRef]
38. Głowacka, K.; Kromdijk, J.; Salesse-Smith, C.; Smith, C.; Driever, S.; Long, S. Is chloroplast size optimal for photosynthetic efficiency? *New Phytol.* **2023**, *239*, 2197–2211. [CrossRef]
39. Paul, P.; Mesihovic, A.; Chaturvedi, P.; Ghatak, A.; Weckwerth, W.; Böhmer, M.; Schleiff, E. Structural and Functional Heat Stress Responses of Chloroplasts of Arabidopsis thaliana. *Genes* **2020**, *11*, 650. [CrossRef]
40. Wang, Q.L.; Chen, J.H.; He, N.Y.; Guo, F.Q. Metabolic reprogramming in chloroplasts under heat stress in plants. *Int. J. Mol. Sci.* **2018**, *19*, 849. [CrossRef]
41. Cai, Y.Q.; Tarin, M.W.K.; Fan, L.L.; Xie, D.J.; Rong, J.D.; He, T.Y.; Chen, L.G.; Zheng, Y.S. Responses of photosynthesis, chloroplast ultrastructure, and antioxidant system of Morinda officinalis how to exogenous 2,4-epibrassinolide treatments under high temperature stress. *Appl. Ecol. Environ. Res.* **2020**, *18*, 3981–4004. [CrossRef]

42. Zhang, L.; Chang, Q.; Hou, X.; Wang, J.; Chen, S.; Zhang, Q.; Wang, Z.; Yin, Y.; Liu, J. The Effect of High-Temperature Stress on the Physiological Indexes, Chloroplast Ultrastructure, and Photosystems of two Herbaceous Peony Cultivars. *J. Plant Growth Regul.* **2023**, *42*, 1631–1646. [CrossRef]
43. Ivanov, A.G.; Velitchkova, M.Y.; Allakhverdiev, S.I.; Huner, N.P.A. Heat stress-induced effects of photosystem I: An overview of structural and functional responses. *Photosynth. Res.* **2017**, *133*, 17–30. [CrossRef] [PubMed]
44. Li, M.; Kim, C. Chloroplast ROS and stress signaling. *Plant Commun.* **2022**, *3*, 100264. [CrossRef] [PubMed]
45. Nishiyama, Y.; Takechi, K.; Nanjo, Y.; Murata, N.; Hayashi, H. Acclimation of photosystem II to high temperature in a suspension culture of soybean (*Glycine max*) cells requires proteins that are associated with the thylakoid membrane. *Photosynth. Res.* **2007**, *90*, 223–232. [CrossRef] [PubMed]
46. Wood, W.; MacGregor-Chatwin, C.; Barnett, S.; Mayneord, G.; Huang, X.; Hobbs, J.; Hunter, C.; Johnson, M. Dynamic thylakoid stacking regulates the balance between linear and cyclic photosynthetic electron transfer. *Nat. Plants* **2018**, *4*, 116–127. [CrossRef] [PubMed]
47. Croce, R.; Carmo-Silva, E.; Cho, Y.B.; Ermakova, M.; Harbinson, J.; Lawson, T.; McCormick, A.J.; Niyogi, K.K.; Ort, D.R.; Patel-Tupper, D.; et al. Perspectives on improving photosynthesis to increase crop yield. *Plant Cell* **2024**, *36*, 3944–3973. [CrossRef]
48. Baker, N.R. Chlorophyll fluorescence: A probe of photosynthesis in vivo. *Annu. Rev. Plant Biol.* **2008**, *59*, 89–113. [CrossRef]
49. Bykowski, M.; Mazur, R.; Wójtowicz, J.; Suski, S.; Garstka, M.; Mostowska, A.; Kowalewska, Ł. Too rigid to fold: Carotenoid-dependent decrease in thylakoid fluidity hampers the formation of chloroplast grana. *Plant Physiol.* **2020**, *185*, 210–227. [CrossRef]
50. Liu, Y.; Ye, J.; Zhu, M.; Atkinson, R.; Zhang, Y.; Zheng, X.; Lu, J.; Cao, Z.; Peng, J.; Shi, C.; et al. Multi-omics analyses reveal the importance of chromoplast plastoglobules in carotenoid accumulation in citrus fruit. *Plant J. Cell Mol. Biol.* **2023**, *117*, 924–943. [CrossRef]
51. Du, X.; Zhang, X.; Wei, Z.; Lei, W.; Hu, G.; Huang, Z.; Kong, L. Photosynthetic characteristics of subtending leaves and their relationships with soybean pod development under heat, drought and combined stresses. *J. Agron. Crop Sci.* **2022**, *209*, 204–215. [CrossRef]